BMB
Reports

BMB Rep.
www.bmbreports.org

The impact of cancer cachexia on gut microbiota composition and short-chain fatty acid metabolism in a murine model

Seung Min Jeong[1,2,#], *Eun-Ju Jin*[3,#], *Shibo Wei*[3], *Ju-Hyeon Bae*[1], *Yosep Ji*[2], *Yunju Jo*[4], *Jee-Heon Jeong*[1], *Se Jin Im*[5,*] *& Dongryeol Ryu*[1,4,*]

[1]Department of Molecular Cell Biology, Sungkyunkwan University School of Medicine, Suwon 16419, [2]HEM Inc., Suwon 16229, [3]Department of Precision Medicine, Sungkyunkwan University School of Medicine, Suwon 16419, [4]Department of Biomedical Science and Engineering, Gwangju Institute of Science and Technology, Gwangju 61005, [5]Department of Immunology, Sungkyunkwan University School of Medicine, Suwon 16419, Korea

This study investigates the relationship between cancer cachexia and the gut microbiota, focusing on the influence of cancer on microbial composition. Lewis lung cancer cell allografts were used to induce cachexia in mice, and body and muscle weight changes were monitored. Fecal samples were collected for targeted metabolomic analysis for short chain fatty acids and microbiome analysis. The cachexia group exhibited lower alpha diversity and distinct beta diversity in gut microbiota, compared to the control group. Differential abundance analysis revealed higher *Bifidobacterium* and *Romboutsia*, but lower *Streptococcus* abundance in the cachexia group. Additionally, lower proportions of acetate and butyrate were observed in the cachexia group. The study observed that the impact of cancer cachexia on gut microbiota and their generated metabolites was significant, indicating a host-to-gut microbiota axis.

INTRODUCTION

Cancer cachexia is a multifactorial disorder that has a characteristic wasting of skeletal muscle mass, and can show a loss of fat mass (1, 2). The muscle wasting induced by cancer cachexia cannot be recovered to a normal or healthy condition by nutritional supplementation, and the damage to muscular function gradually becomes worse. This is because of an unbalanced protein metabolism that breaks down too much muscle, and reduced food intake (3).

*Corresponding authors. Dongryeol Ryu, Tel: +82-62-715-5374; Fax: +82-62-715-5309; E-mail: dryu@gist.ac.kr; Se Jin Im, Tel: +82-31-299-6125; Fax: +82-31-299-6029; E-mail: sejinim@skku.edu
#These authors contributed equally to this work.

https://doi.org/10.5483/BMBRep.2023-0068

Received 25 April 2023, Revised 30 April 2023, Accepted 14 May 2023, Published online 26 May 2023

Keywords: 16s amplicon sequencing, Cancer cachexia, Gut microbiome, Muscle atrophy, Short-chain fatty acids (SCFA)

Major symptoms of cancer cachexia include the involuntary and progressive loss of muscle mass, loss of appetite (anorexia), systemic inflammation, and unbalanced hepatic glucose and lipid metabolism, with or without the loss of adipose tissue mass (4). The crucial mechanism of cancer cachexia is the up-regulated catabolism of muscular protein, followed by down-regulated protein synthesis, causing loss of lean body mass (5).

About half of all patients suffering from cancer are finally expected to progress toward a cancer cachexia (4). For patients having cancer, up to one-third of deaths are caused by a cancer cachexia (5). The prevalence of cachexia, a syndrome marked by extreme weight loss and muscle wasting, varies depending on the patient's condition; it ranges 5-15% in patients with end-stage chronic heart failure, to 50-80% in those with advanced malignant cancer (6). Cachexia is a well-known condition that affects patients with various chronic illnesses, including chronic kidney disease, chronic obstructive pulmonary disease (COPD), neurological diseases, and rheumatoid arthritis. Cachexia is associated with high mortality rates, with severe COPD patients having a mortality rate of 15-25% per year, while chronic heart failure and CKD patients have a mortality rate of 20-40% per year. Cancer cachexia patients have the highest mortality rate, with 20-80% per year. The prevalence of cachexia is increasing in industrialized countries due to the rising incidence of chronic illnesses. Globally, it is estimated that 1.5-2 million people die with cachexia per year. As cachexia shows high prevalence and mortality, academic developments through research and methods of properly treating cachexia are required for patients worldwide (6).

Recent studies have provided evidence linking the gut microbiota to numerous diseases (7, 8). Recent study has demonstrated the impact of gut microbiota on the function and mass of skeletal muscle in mice (9). The research discovered that in germ-free (GF) mice, there was a presence of muscle atrophy accompanied by the reduced expression of key genes involved in the assembly and functioning of the neuromuscular junction, including insulin-like growth factor 1, Rapsyn, and Lrp4. These findings indicate the importance of gut microbiota in maintaining proper muscle structure and neuromuscular junction

ISSN: 1976-670X (electronic edition)

integrity. Additionally, GF mice showed reduced serum choline levels, which is the precursor of acetylcholine, a neurotransmitter that plays a critical role in mediating signals at neuromuscular junctions. Interestingly, fecal microbiota transplantation from non-GF mice resulted in an increase in skeletal muscle mass, decreased muscle atrophy markers, and elevated expression of Rapsyn and Lrp4 involved in the formation of neuromuscular junction (9).

In a recent study (10), the gut microbiota from a murine obese model induced a more significant gain in body weight when transplanted into a germ-free (GF) mouse, than the gut microbiota from a lean mouse. This research implies that the gut microbiota may play a role in the development of obesity. The obese have been shown to have a lower prevalence of Bacteroidetes and a higher prevalence of Firmicutes, indicating compositional differences in the gut microbiota that lead to increased energy utilization and stimulation of lipogenesis (11). In contrast, GF lean mice did not become obese on a high calorie diet, and showed an increase in skeletal muscle and phosphorylated adenosine monophosphate-activated protein kinase (AMPK), which leads to a reduction in malonyl-CoA levels and an increase in fatty acid oxidation (12). Additionally, lipopolysaccharide (LPS) has been shown to trigger chronic inflammation in mice (13), and is associated with metabolic disease and inflammation (14). Various opinions have been offered to link with age-related upregulation of inflammatory state, including the impaired homeostasis of gut microbiota. This was associated with increased levels of circulating endotoxin, like Lipopolysaccharide.

RESULTS

Establishment and validation of a cancer cachexia-induced murine model

To validate our hypothesis, we initially established a cancer cachexia model in mice by transplanting Lewis lung cancer (LLC) cells, following the sequence shown in Fig. 1A. On day 30 of cancer cachexia induction, we euthanized the mice and examined relevant tissues, including skeletal muscle and adipose tissue, to assess cachexia development. During necropsy, we observed the absence of epididymal fat in cachexia mice (Supplementary Fig. 1A of the Supplementary Information (SI)). Both cancer-free body weight and total body weight were reduced (Supplementary Fig. 1B, C of the SI), confirming the presence of anorexia, a common symptom associated with cachexia (Supplementary Fig. 1D of the SI). The mass of all measured skeletal muscles, including tibialis anterior (TA), gastrocnemius, soleus, quadriceps, and extensor digitorum longus (EDL), was diminished (Fig. 1B-D, and Supplementary Fig. 1E-P of the SI). However, when normalized to cancer-free body weight, no decrease was observed in the EDL and soleus muscles (Supplementary Fig. 1I, O). Additionally, a noticeable trend of decreased dry brachial muscle mass was observed (Supplementary Fig. 1Q-S of the SI). Moreover, there was a substantial loss of visceral fat (Supplementary Fig. 1T-V of the SI). Consistent with these findings, we observed a significant reduction in muscle strength in mice with induced cancer

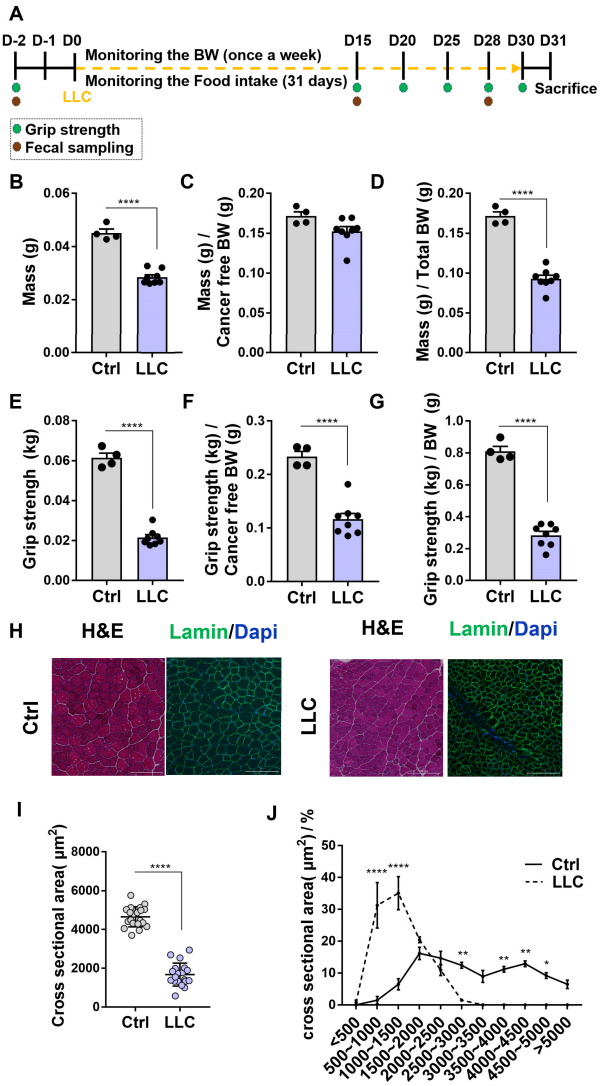

Fig. 1. Cachexia phenotype of Lewis lung carcinoma-bearing (LLC)-allografted mice. (A) Timeline of the LLC-induced cachexia mouse model. (B-D) The absolute mass, the normalized mass with the cancer-free body weight, and the normalized mass with the cancer-free body weight of tibialis anterior (TA) muscles. (E-G) The grip strength without normalization and with normalization either the cancer free body weight or body weight. (H) The H&E and lamin/Dapi stains of cross-sectional TA muscles. (I) Scatter plot showing cross-sectional areas (CSA) of TA muscles. (J) Myofiber size (CSA) distribution of TA muscles. All values in (B-G, I and J) are represented as mean ± standard deviation, and the P-values were determined by Mann-Whitney test (B-G), student's t test (I) and two-way ANOVA followed by Tukey's test. P-values of < 0.05 (*), < 0.01 (**), and < 0.0001 (****) were considered statistically significant.

cachexia. Finally, histological analysis confirmed the presence of muscle wasting, conclusively indicating the development of cancer cachexia in these mice (Fig. 1H-J).

Gut microbiota diversity analysis reveals significant differences between control and cachexia-induced murine models

There are several measures of alpha diversity, including Chao, ACE, and Shannon, that assess the richness and evenness of the gut microbiota. In this study, the Shannon index showed a higher alpha diversity in the control group compared to the cachexia-induced group, while the richness indices were slightly higher or similar in the control group (Fig. 2B). Beta diversity was evaluated using principal coordinate analysis (PCoA) with Bray-Curtis dissimilarity, which showed that samples from the control group were clustered together on the left side of the plot, while samples from the cachexia-induced group were grouped on the right side. This indicates that the gut microbiota composition was similar within each group, but distinct between groups, with the composition of the cachexia-induced group significantly different from that of the control group (Fig. 2C).

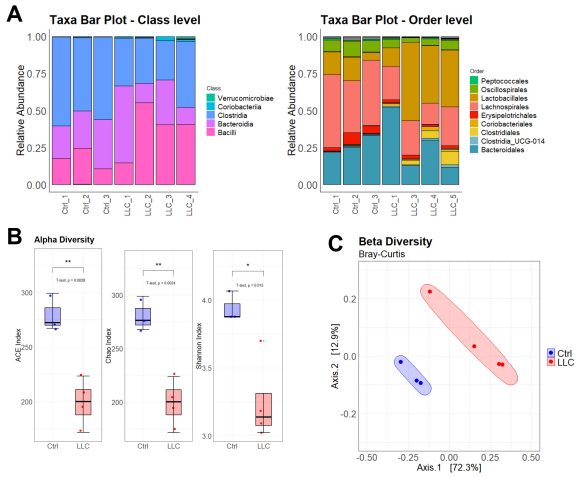

Fig. 2. Illustrates the differences in microbial composition and diversity between the control group and the group induced with cancer cachexia. (A) The relative abundance of microbial classes and orders in the murine gut is depicted. (B) The alpha diversity of fecal microbiome from mice, measured using the ACE, Chao, and Shannon indices. The cancer cachexia group (LLC_D30) exhibited lower alpha diversity compared to the control group (Ctrl_D30). The boxplots represent the 25th quartile, median, and 75th quartile values. Statistical significance was determined using the Mann-Whitney test (B), with P-values < 0.05 (*) and < 0.01 (**) considered significant. (C) The beta diversity of fecal samples through Principal Coordinates Analysis with Bray-Curtis dissimilarity. The plot on the right side shows that the gut microbiota composition of the cancer cachexia group (LLC_D30) was distinctly different from that of the healthy control group (Ctrl_D30).

Differential abundance analysis of gut microbiota by DESeq2 confirmed the deficiency of beneficial bacteria in the cachexia-induced group

The results of the DESeq2 analysis revealed significantly differential abundance of bacteria between the cancer cachexia-induced group and control group, as illustrated in the volcano plot (Fig. 3A). The red points in the plot represent significantly differential taxa of bacteria between the groups (P value $<$ 0.05) by DESeq2, where points on the left side of the plot in negative log2 fold change mean more abundance in the control group, and *vice versa*. These bacteria include *Bifidobacteriaceae Bifidobacterium*, *Peptostreptococcaceae Romboutsia*, *Streptococcaceae Streptococcus*, and *Eggerthellaceae Raoultibacter*. The rarefied counts of genus *Bifidobacterium* and genus *Romboutsia* in the control group were significantly higher than that of the cachexia-induced group (Fig. 3B). In particular, genus Bifidobacterium is generally considered a beneficial bacterium that is abundant in a healthy gut microbiota. Moreover, the rarefied counts of genus Streptococcus in the control group were much lower than that of the cachexia-induced group (Fig. 3B). The bar plots show the log2 fold change of rarefied counts and the names of microbes that had significant differential abundance in each group by DESeq2 analysis (Fig. 2B). Additionally, the box plots compare the relative abundance of some microbes (Fig. 3C).

Differential abundance of gut microbial metabolites between the healthy and cachexia-induced mice

The fecal concentrations of SCFAs, including acetate, propionate, and butyrate, were analyzed in the cachexia-induced and control groups using gas chromatography with a flame ionization detection (GC-FID) system (Fig. 4). Propionate was found to be significantly more abundant in the cachexia-induced group, while butyrate was notably higher in the control group, in terms of the molar ratios of SCFAs. Additionally, in terms of SCFA concentration (mM), acetate was more abundant in the control group, and butyrate was also significantly more abundant in the control group. These findings are consistent with previous studies that suggest that a higher abundance of SCFAs is indicative of a healthier gut microbiota (15).

DISCUSSION

The use of LLC cell allografts successfully induced cancer cachexia in mice, resulting in a decrease in muscle weight and an increase in spleen volume, which confirm the establishment of the cachexia condition. To understand the impact of cancer cachexia on gut microbiota, we analyzed fecal samples from the mice using 16S amplicon sequencing and GC-FID metabolite analysis.

The presence of cancer cachexia condition was found to significantly decrease the alpha diversity indices of gut microbiota, compared to the control group. Furthermore, analysis of beta diversity through PCoA using the Bray-Curtis dissimilarity

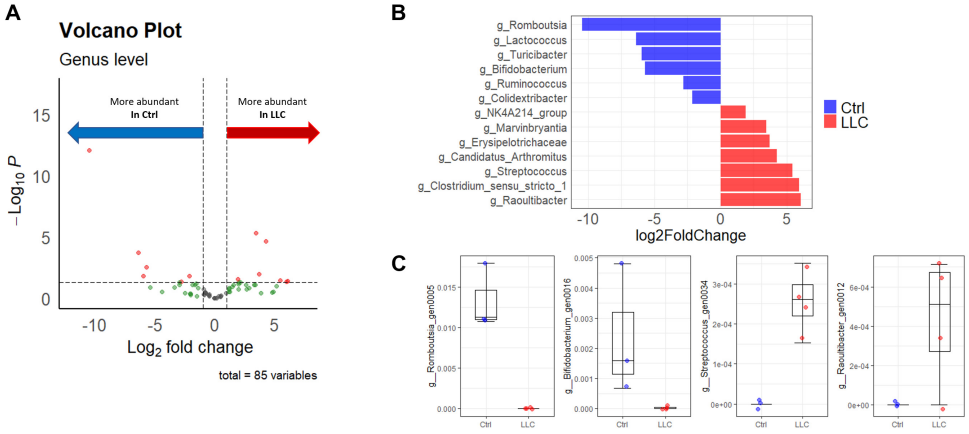

Fig. 3. Differential abundance analysis of gut microbiota by DESeq2. (A) Result of DESeq2 analysis illustrated in volcano plot showing significantly differential abundance of bacteria between cancer cachexia induced group (LLC_D30) and control group (Ctrl_D30). (B) Microbes of significantly different abundance in genus level by DESeq2 analysis between groups expressed in log2 fold change. (C) Representative microbes of significantly difference in abundance by DESeq2 are illustrated in each box plot showing the 25th quartile, median, and 75th quartile values.

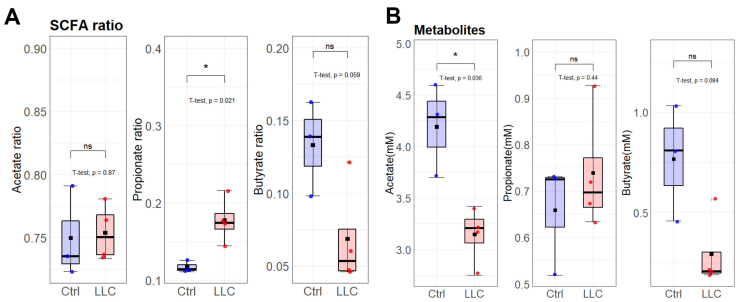

Fig. 4. Concentration and molar ratio of gut microbial metabolites (SCFA) detected by GC-FID in mouse fecal samples. (A) The molar ratios of major SCFA metabolites are compared. The molar ratio of propionate is significantly lower in the control group, while the molar ratio of butyrate is notably higher in the control group. (B) The concentration (mM) of acetate in the control group is significantly higher, and the concentration of butyrate is also notably higher in the control group. Statistical significance was determined using the Mann-Whitney test with P-values $<$ 0.05 (*) considered significant.

index showed a noticeable shift in the composition of gut microbiome between the two groups. In particular, the abundance of certain bacteria, such as Bifidobacterium, which are typically considered beneficial, was significantly reduced in the cachexia-induced group. Additionally, the concentrations of gut microbial metabolites, such as acetate and butyrate, which are indicative of a healthy gut microbiota, were found to decrease in the cancer cachexia-induced group. These results suggest that the physiopathologic state of the host can influence gut microbial diversity and the metabolites they produce. Our study also provides a basis for future research to create insights into the impact of cancer cachexia on the gut microbiota in terms of gut microbial composition and metabolites.

This study examines how LLC cancer cell allografts impact the development of cancer cachexia, and the changes in gut microbiota composition and metabolites. However, the limited number of mice used in this study emphasizes the need for larger cohorts in future research to establish more conclusive findings. Furthermore, the study did not determine whether host-derived metabolites (e.g., lactate) or specific cytokines or hormones associated with cachexia and inflammatory responses (e.g., GDF15) directly affect the gut microbiota (16, 17). Hence, it is crucial to conduct future studies to investigate the effects of these metabolites or cytokines on the diversity of gut microbial communities. Additionally, since this study was conducted on mice, it is imperative to conduct further research on cachexia patients to ascertain its relevance to human health. Moreover, exploring alterations in gut microbiota and short-chain fatty acids (SCFA) in other types of cachexia, such as chronic kidney disease, where blood lactate levels are not expected to

change, would be intriguing.

Finally, based on the findings of this study, the administration of probiotics as a preventive or curative measure for cancer cachexia is a potential approach to modulating the intestinal microbiota environment. Therefore, exploring the potential of administering probiotics merits further investigation as a novel approach to treating cancer cachexia.

MATERIALS AND METHODS

Cancer cachexia model grip strength

All animal procedures conducted in this study were approved and reviewed by the Institutional Animal Care and Research Advisory Committee at the Laboratory Animal Research Center, Sungkyunkwan University School of Medicine (SKKUIACUCU 2021-04-17-1). To establish a Cancer Cachexia model, male C57BL/6 mice, aged 10 weeks, were used, and the induction of the condition was achieved by administering LLC cells. The LLC cells were cultured in Dulbecco modified Eagles medium including 10% FBS and 1% penicillin and streptomycin at 37 degrees Celsius with 5% CO2. Prior to injection of the LLC cells into the mice, the cells were counted and resuspended at 1×10^7 cells/ml in sterilized PBS. The mice were anesthetized using 3% isoflurane, and 100 µl of LLC cells (1.0×10^6 cells) were implanted subcutaneously in the back flanks of the mice. The size of the tumor was measured using a caliper, and the tumor volume was calculated using the formula: $0.5 \times (\text{length} \times \text{width}^2)$. The mice's body weight and food intake were measured every other day.

Grip strength

The grip strength of mice was assessed using a grip strength meter (JENOG DO BIO & PLANET CO., LTD, Seoul, Korea). Each mouse was placed on the grid, allowing the forelimb and hindlimb to grasp it. A gentle and constant force was applied to the tail until the forelimb and hindlimb separated from the grid. The peak maximum force in kilograms was recorded on the grip strength meter. The grip strength measurements were performed 15 times in total, divided into 3 sets of 5 repetitions each. After every 5 repetitions, a 2-minute break was provided. The three highest grip strength values were used for further analysis.

Tissue preparations, histology, and immunohistochemistry

Muscles isolated from the mice were embedded using Tissue-Tek OCT compound (Sakura) and cut into 5 µm thick serial sections using a cryomicrotome. For the analysis of muscle structure and fibrosis, the muscle sections were stained with Harrys hematoxylin (YD Diagnostics) and eosin (Polysciences) following the manufacturer's protocol. Images were captured using a Leica APERIO CS2 slide scanner. To measure the cross-sectional area, muscle sections underwent fixation, permeabilization, and blocking steps. Subsequently, the sections were incubated overnight with a primary antibody against laminin (ab11575, 1:500, Abcam) and then with the secondary antibody for 1 hour and 30 minutes (Thermo Fisher). Images were captured and processed using a Nikon ECLIPSE TE = 20,000 U inverted microscope with NIS-ELEMENTS F software (Nikon). The cross-sectional area was measured using ImageJ software (https://imagej.nih.gov/).

Composition of dataset

Objective of this experiment is to compare between mouse feces of control group and those of cancer cachexia-induced group. Cancer cachexia-induced group was composed of 4 mice and control mouse group was also composed of 3 mice. Sample of mouse feces were collected periodically in Day 0 and Day 30 in this experiment. In the beginning point (Day 5), fecal samples of 5 mice are randomly collected out of total mouse group before inducing cancer cachexia. After that, Cachexia-induced mouse group was allografted with LLC cells in the epidermis to induce cancer cachexia, resulting loss of muscle mass. Control group is injected with Phosphate Buffered Saline (PBS) instead of LLC cells. Body weight was measured every 5 days from Day 0 to Day 30, and amount of food intake were measured every 10 days. In Day 30, all mice are sacrificed to measure Gastrocnemius (GAS) and Tibialis Anterior (TA) muscle weight and size of spleen, adipose tissue and other phenotypical traits. Fecal samples of Day 30 were used to compare results between Cancer cachexia-induced group and Control group.

Metagenomic analysis

To practice metagenomic analysis, DNA of mouse fecal samples was extracted by using commercial DNA extraction kit (MagBind® Environmental DNA 96 Kit, M5645-01, OMEGA, USA). Extraction protocol was operated as standard manual of manufacturer. After extraction of DNA, V3-V4 region of 16s rRNA in the samples was amplified for 16s amplicon sequencing using the primer (341F: 5'-CCTACGGGNGGCWGCAG, 805R: 5'-GACTACHVGGGTATCTAATCC). According to 16s rRNA amplicon sequencing protocol of the Illumina MiSeq® System, indexing and library preparation of the samples was processed and 16s rRNA amplicon sequencing was conducted using the sequencer (MiSeq® System, Illumina, USA). Paired end sequencing outputs are merged, denoised and removed of chimera sequence by DADA2 pipeline of Qiime2 (Qiime2, ver. 2019-4). ASV feature table of the samples is retrieved by taxonomy classification based on Silva 138 16s rRNA database. ASV feature table, taxonomy classification file and taxonomic tree information file (mafft-fasttree) are imported using 'phyloseq' package of R program for further metagenomic analysis.

Analysis of targeted metabolites

Collect 70 mg of each mouse fecal sample and mix and vortex with 1 ml of diluted water. Centrifuge 1,000-2,000 × g for 1 min at room temperature and take 150 µg of supernatant to each glass vial for Gas Chromatography (GC) analysis. Make

GC buffer with NaCl 33%, phosphoric acid 0.005% and add 150 µl of GC buffer to glass vial. Vortex GC vials sufficiently and stabilize the solution for 1 hour at room temperature. Analyze each sample of 300 µl solution in GC vials with GC/flame ionization detector (GC-FID: Agilent 7890B, Agilent Technologies, USA) and measure the targeted metabolites, which is short chain fatty acids, of each sample.

Statistical analysis

Taxonomic classification results at genus level were used to conduct differential abundance analysis (DAA) and to compare alpha-diversity, beta-diversity. Rarefaction at the minimum sequence reads (12,817) was processed to normalize different sequencing depth between samples and to correct the bias derived from different sequencing depth of samples. DESeq2 algorithm was used as a method of DAA to detect specific bacteria that shows statistically different in abundance between control group and cachexia-induced group. Box plots of alpha diversity, taxonomic abundance (genus level), concentration of short chain fatty acid and PCoA plots of beta diversity were created through ggplot2 package of R program. Statistical significance (P-value) was calculated by non-parametric Wilcoxon signed-rank test or unpaired T-test depending on the normality confirmed by Shapiro-Wilk test and P-value of less than 0.05 was regarded as statistically significant.

ACKNOWLEDGEMENTS

This study was supported by the National Research Foundation of Korea (NRF) funded by the Ministry of Science and ICT (2023R1A2C3006220 and 2021R1A5A8029876 to D.R.), a "GIST Research Institute (GRI) IIBR" grant funded by the GIST in 2023 (to D.R.), and HEM Inc. We would like to appreciate all lab members of Ryu lab.

CONFLICTS OF INTEREST

The authors declare no competing financial interests, except S.M.J. and Y.J., who are employee of HEM Pharma Inc.

REFERENCES

1. Jo Y, Yeo MK, Dao T, Kwon J, Yi HS and Ryu D (2022) Machine learning-featured Secretogranin V is a circulating diagnostic biomarker for pancreatic adenocarcinomas associated with adipopenia. Front Oncol 12, 942774
2. Lee JY, Hong N, Kim HR et al (2018) Effects of serum albumin, calcium levels, cancer stage and performance status on weight loss in parathyroid hormone-related peptide positive or negative patients with cancer. Endocrinol Metab (Seoul) 33, 97-104
3. Fearon K, Strasser F, Anker SD et al (2011) Definition and classification of cancer cachexia: an international consensus. Lancet Oncol 12, 489-495
4. Aoyagi T, Terracina KP, Raza A, Matsubara H and Takabe K (2015) Cancer cachexia, mechanism and treatment. World J Gastrointest Oncol 7, 17
5. Ahmed DS, Isnard S, Lin J, Routy B and Routy J-P (2021) GDF15/GFRAL pathway as a metabolic signature for cachexia in patients with cancer. J Cancer 12, 1125
6. von Haehling S, Anker MS and Anker SD (2016) Prevalence and clinical impact of cachexia in chronic illness in Europe, USA, and Japan: facts and numbers update 2016. J Cachexia Sarcopenia Muscle 7, 507-509
7. Kang BE, Park A, Yang H et al (2022) Machine learning-derived gut microbiome signature predicts fatty liver disease in the presence of insulin resistance. Sci Rep 12, 21842
8. Lo Sasso G, Ryu D, Mouchiroud L et al (2014) Loss of Sirt1 function improves intestinal anti-bacterial defense and protects from colitis-induced colorectal cancer. PLoS One 9, e102495
9. Lahiri S, Kim H, Garcia-Perez I et al (2019) The gut microbiota influences skeletal muscle mass and function in mice. Sci Transl Med 11, eaan5662
10. Turnbaugh PJ, Ley RE, Mahowald MA, Magrini V, Mardis ER and Gordon JI (2006) An obesity-associated gut microbiome with increased capacity for energy harvest. Nature 444, 1027-1031
11. Turnbaugh PJ, Bäckhed F, Fulton L and Gordon JI (2008) Diet-induced obesity is linked to marked but reversible alterations in the mouse distal gut microbiome. Cell Host Microbe 3, 213-223
12. Abu-Elheiga L, Oh W, Kordari P and Wakil SJ (2003) Acetyl-CoA carboxylase 2 mutant mice are protected against obesity and diabetes induced by high-fat/high-carbohydrate diets. Proc Natl Acad Sci U S A 100, 10207-10212
13. Cani PD, Amar J, Iglesias MA et al (2007) Metabolic endotoxemia initiates obesity and insulin resistance. Diabetes 56, 1761-1772
14. Grosicki GJ, Fielding RA and Lustgarten MS (2018) Gut microbiota contribute to age-related changes in skeletal muscle size, composition, and function: biological basis for a gut-muscle axis. Calcif Tissue Int 102, 433-442
15. Canani RB, Di Costanzo M, Leone L, Pedata M, Meli R and Calignano A (2011) Potential beneficial effects of butyrate in intestinal and extraintestinal diseases. World J Gastroenterol 17, 1519
16. Moon JS, Goeminne LJE, Kim JT et al (2020) Growth differentiation factor 15 protects against the aging-mediated systemic inflammatory response in humans and mice. Aging Cell 19, e13195
17. Han JH, Kim M, Kim HJ et al (2021) Targeting lactate dehydrogenase A with catechin resensitizes SNU620/5FU gastric cancer cells to 5-fluorouracil. Int J Mol Sci 22, 5406